



CHORUS

This is the accepted manuscript made available via CHORUS. The article has been published as:

Magnetic Cycloid of BiFeO_3 from Atomistic Simulations

D. Rahmedov, Dawei Wang, Jorge Íñiguez, and L. Bellaiche

Phys. Rev. Lett. **109**, 037207 — Published 20 July 2012

DOI: [10.1103/PhysRevLett.109.037207](https://doi.org/10.1103/PhysRevLett.109.037207)

Magnetic cycloid of BiFeO₃ from atomistic simulations

D. Rahmedov¹, Dawei Wang², Jorge Íñiguez³ and L. Bellaiche¹

¹*Physics Department and Institute for Nanoscience and Engineering,
University of Arkansas, Fayetteville, Arkansas 72701, USA*

²*Electronic Materials Research Laboratory,
Key Laboratory of the Ministry of Education
and International Center for Dielectric Research,
Xi'an Jiaotong University, Xi'an 710049, China*

³*Institut de Ciència de Materials de Barcelona (ICMAB-CSIC),
Campus UAB, 08193 Bellaterra (Barcelona), Spain*

Abstract

An effective Hamiltonian is developed to investigate the magnetic cycloid of BiFeO₃ (BFO) multiferroic. This approach reproduces many complex features of this cycloid, such as its plane of rotation containing the polarization and the newly discovered spin density waves resulting from the canting of magnetic dipoles *out* of this cycloidal plane. It also suggests that the energetic origin of the cycloid can be thought as the *converse* spin-current model, and reveals the mechanisms responsible for the spin density waves. Finally, this atomistic scheme resolves an ongoing controversy about the cycloid anharmonicity, and revisits a recent misconception about the relationship between out-of-plane spin-density waves and the weak magnetization associated with the spin-canted structure of BFO.

PACS numbers: 75.25.-j, 75.40.Mg, 75.30.Fv, 77.80.-e

Multiferroic materials have recently recaptured the attention of many researchers, because of the inherent coupling between their magnetic order and ferroelectricity [1–3]. In particular, BiFeO₃ has been intensively studied since it is one of the few multiferroics for which magnetic order and an electric polarization coexist at room temperature (see, e.g., Refs. [4–12] and references therein). Interestingly, the magnetic order of bulk BFO is rather complex and even controversial. While it has been known for some years that such order consists of a cycloid with the magnetic dipoles rotating within a plane containing the polarization [6, 13, 14], there has been contradictory reports about the degree of anharmonicity of this cycloid [15–21]. More importantly, a recent measurement found an unexpected *additional* spin density wave (SDW) that makes the magnetic dipoles canting *out* of the cycloidal plane [22]. This breakthrough naturally raises the question of whether the energy expressions used so far to explain the origin of the magnetic cycloid in BFO [23–25] are in fact incorrect since none of them have resulted in the prediction of an out-of-plane SDW. If that is indeed the case, one may wonder what is the real energetic origin of such cycloid and what are the mechanisms responsible for the out-of-plane SDW that coexists with the in-plane rotation of the magnetic dipoles. Other important questions to resolve or revisit in BFO are the possible destruction of this cycloid in favor of a spin-canted structure when applying a magnetic field [26], and the relationship (if any) between the out-of-plane SDW inherent to the cycloid and the weak ferromagnetic (FM) vector inherent to the spin-canted structure [10, 12, 22]. In this Letter, all the aforementioned issues are addressed and resolved, via the use and development of an effective Hamiltonian technique.

In our model, the total internal energy, E_{tot} , is written as a sum of two terms, $E_{\text{FE-AFD}}(\{\mathbf{u}_i\}, \{\eta\}, \{\omega_i\})$ and $E_{\text{MAG}}(\{\mathbf{m}_i\}, \{\mathbf{u}_i\}, \{\eta\}, \{\omega_i\})$. \mathbf{u}_i is the local soft mode in unit cell i , which is directly proportional to the electric dipole moment centered on the Fe ion of that cell. $\{\eta\}$ is the strain tensor, that gathers homogeneous and inhomogeneous contributions [30]. ω_i is a pseudo-vector characterizing the oxygen octahedra tilting – also termed the antiferrodistortive (AFD) distortions – in unit cell i . It is centered on Fe ions too, and its direction provides the axis about which the oxygen octahedra tilt while its magnitude gives the angle of that tilt [31]. \mathbf{m}_i is the magnetic dipole moment centered on the Fe-site i and is assumed to have a fixed magnitude of $4\mu_B$, as consistent with first principles [4] and measurements [32]. $E_{\text{FE-AFD}}$ is given in Ref. [31] and involves terms associated with ferroelectricity, strain and AFD distortions, and their mutual couplings. E_{MAG} gathers

magnetic degrees of freedom and their couplings, and is proposed here to be:

$$\begin{aligned}
E_{\text{MAG}}(\{\mathbf{m}_i\}, \{\mathbf{u}_i\}, \{\eta\}, \{\omega_i\}) = & \sum_{i,j,\alpha,\gamma} Q_{ij,\alpha\gamma} m_{i,\alpha} m_{j,\gamma} + \sum_{i,j,\alpha,\gamma} D_{ij,\alpha\gamma} m_{i,\alpha} m_{j,\gamma} \\
& + \sum_{i,j,\alpha,\gamma,\nu,\delta} E_{ij,\alpha\gamma\nu\delta} m_{i,\alpha} m_{j,\gamma} u_{i,\nu} u_{i,\delta} + \sum_{i,j,\alpha,\gamma,\nu,\delta} F_{ij,\alpha\gamma\nu\delta} m_{i,\alpha} m_{j,\gamma} \omega_{i,\nu} \omega_{i,\delta} \\
& + \sum_{i,j,l,\alpha,\gamma} G_{ij,l,\alpha\gamma} \eta_l(i) m_{i,\alpha} m_{j,\gamma} + \sum_{i,j} K_{ij} (\omega_i - \omega_j) \cdot (\mathbf{m}_i \times \mathbf{m}_j) - \sum_{i,j} C_{ij} (\mathbf{u}_i \times \mathbf{e}_{ij}) \cdot (\mathbf{m}_i \times \mathbf{m}_j) \quad (1)
\end{aligned}$$

where α , γ , ν and δ denote Cartesian components, and $\eta_l(i)$ is the l^{th} component of the strain tensor at the site i . The index i runs over all the Fe-sites. The first term of Eq. (1) corresponds to the dipolar interactions between magnetic moments, with j running over *all* the Fe-sites [30]. The second term has the same analytical expression than the first one but corresponds to a different energy: it represents the (short-range) exchange interactions. The third, fourth and fifth energies characterize how the local soft-modes, AFD degrees of freedom and strain affect such exchange interactions, respectively [11, 33]. The j index for the second, third, fourth, and fifth energies runs over the first, second and third nearest neighbors of the Fe-site i . Note that the analytical expression of the third, fourth and fifth terms are associated with the lowest possible orders in the couplings, because our reference state is cubic. The sixth energetic term of Eq. (1) has been recently proposed to explain and reproduce the spin-canted, weak ferromagnetic structure of BFO compounds [12]. In this term, j only runs over the (six) first nearest neighbors of the Fe-site i . It is important to realize that this term involves the AFD distortions at sites i and j (and not the local electric dipoles), indicating that the spin-canted structure of BFO originates from the tilting of the oxygen octahedra (rather than being induced by the electrical polarization) – as consistent with first-principles computations [10, 12]. The novelty of the present approach with respect to Ref. [12] resides in the last term of Eq. (1). As we will see, the introduction of this term leads to the activation of the observed magnetic cycloid of BFO, with its complex features being all qualitatively reproduced. In this last term, j only runs over the twelve Fe sites that are second-nearest neighbors of the Fe-site i , and \mathbf{e}_{ij} is a vector (of $\sqrt{2}$ length in reduced units) along the direction joining the Fe-sites i and j . This term, unlike the sixth energy of Eq. (1), involves the electric dipoles since it depends on \mathbf{u}_i . The $D_{ij,\alpha\gamma}$, $E_{ij,\alpha\gamma,\nu,\delta}$, $F_{ij,\alpha\gamma,\nu,\delta}$ and $G_{ijl,\alpha\gamma}$ and K_{ij} parameters entering Eq. (1) are extracted from first-principles calculations on small cells [11, 12, 33]. On the other hand, the C_{ij} coefficient is allowed to vary here to determine its effect on magnetic properties.

The E_{tot} total internal energy is used in Monte-Carlo (MC) simulations on a $18 \times 18 \times 18$ supercell, with up to 1 million MC sweeps, to obtain finite-temperature properties of bulk BFO [34]. This effective Hamiltonian provides a Curie temperature of around $T_C \simeq 1080$ K below which bulk BFO adopts a $R3c$ state that exhibits a polarization pointing along the [111] pseudocubic direction and oxygen octahedra tilting in anti-phase fashion about this same [111] direction. Such predictions are consistent with experiments [9, 35, 36]. Moreover, a magnetic order develops below $T_N \simeq 650$ K when using the proposed total energy, which is also in excellent agreement with the measured critical temperature $\simeq 625\text{K}-643\text{K}$ [32, 35].

When the C_{ij} parameter of Eq. (1) is below a critical value of $\simeq 3 \times 10^{-6}$ Hartree/(Bohr μ_B^2) at 1K, the magnetic structure consists of a spin-canted structure for which a strong G-type antiferromagnetic (AFM) vector coexists with a weak ferromagnetic vector, with these two vectors being perpendicular to each other and lying on the (111) plane. Such findings are consistent with Refs. [10, 12]. On the other hand, a complex magnetic cycloid develops for C_{ij} larger than this critical value [37]. Figures 1 display a snapshot of this cycloid for $C_{ij} = 5 \times 10^{-6}$ Hartree/(Bohr μ_B^2) at a temperature $T=0.2\text{K}$. This cycloid propagates along $[0\bar{1}1]$, that is a pseudo-cubic direction joining Fe ions being second nearest neighbors of each other and that is perpendicular to the polarization, \mathbf{P} , in agreement with measurements [6, 13, 14, 18, 22]. This cycloid can be thought as a superposition of two simultaneous waves: one “in-plane” wave for which the projection of the magnetic dipoles on the $(\bar{2}11)$ cycloidal plane rotates between the $[0\bar{1}1]$ and $[111]$ direction when moving along the propagation direction, see Figure 1a; and an “out-of-plane” wave for which the magnetic dipoles also possess a component being *normal* to the cycloidal plane, with these out-of-plane components changing their values and even their signs [that is, they cross the $(\bar{2}11)$ plane] when moving along the propagation direction, see Fig. 1b. Interestingly, the “in-plane” cycloidal structure has been previously observed by various groups for some time [6, 13, 14, 18] while the additional out-of-plane wave has just been recently evidenced [22]. Moreover, these out-of-plane components are rather small with respect to the in-plane components (their maximum value in Fig. 1b is about $0.5 \mu_B$, while the magnitude of the magnetic moment on each Fe ions is $4\mu_B$). As a result, the magnetic dipoles deviate by less than 5 degree from the $(\bar{2}11)$ cycloidal plane, when choosing $C_{ij} = 5 \times 10^{-6}$ Hartree/(Bohr μ_B^2) and $T=0.2\text{K}$ (see Fig. 2). Such predictions are fully consistent with the experiment of Ref. [22]. Figures 1 and 2 also reveal that these out-of-plane components are maximum

in magnitude when the in-plane components of the magnetic dipoles are almost parallel or antiparallel to the polarization (along $[111]$). Conversely, these out-of-plane components nearly vanish when the magnetic moments lie along the cycloid propagation direction (along $[0\bar{1}1]$). We also numerically found (not shown here) that the spins cant more and more (respectively, less and less) out of the cycloidal plane when the temperature is increased for a given C_{ij} coefficient (respectively, when C_{ij} further increases at a fixed temperature).

To understand the origin of such out-of-plane modulation, we compared the total internal energy of the magnetic structure shown in Figs. 1 with that of the *purely in-plane cycloidal magnetic structure*. These calculations indicated that the last term of Eq. (1) *disfavors* the formation of an out-of-plane spin wave. Rather, we found that it is the magnetic exchange interactions that energetically leads to the activation of these out-of-plane waves, once the in-plane cycloidal magnetic structure occurs.

To further characterize the complex magnetic structure of BFO bulks, we computed the Fourier transform of the local magnetic dipoles' configuration for the different reciprocal k-points allowed for the $18 \times 18 \times 18$ supercell [38]. The reciprocal k-vector possessing the largest magnitude of these Fourier transforms is given by $\mathbf{k}_{\text{cyclo}} = \frac{2\pi}{18a_{\text{lat}}} (9\mathbf{x} - 8\mathbf{y} + 8\mathbf{z})$, where a_{lat} is the lattice constant of the 5-atom primitive cell and where \mathbf{x} , \mathbf{y} and \mathbf{z} are unit vectors along the pseudo-cubic $[100]$, $[010]$ and $[001]$ directions, respectively. $\mathbf{k}_{\text{cyclo}}$ characterizes the modulation period and propagation direction of the mimicked cycloid [6, 13, 14, 18]. The square of its Fourier component is rather large: it contains 99.12 % of the total spectra gathering the Fourier transforms at all possible k-points, when $C_{ij} = 5 \times 10^{-6}$ Hartree/(Bohr μ_B^2) at 5K. Interestingly, a second reciprocal vector, \mathbf{k}_{anh} , also possesses a significant square of its Fourier component – that is of the order of 0.09% for that C_{ij} and temperature. This vector is $\mathbf{k}_{\text{anh}} = \frac{2\pi}{18a_{\text{lat}}} (9\mathbf{x} - 6\mathbf{y} + 6\mathbf{z})$. As consistent with Ref. [18], its existence indicates that the cycloid exhibits some *anharmonicity*. In fact, the ratio of 99.12% over 0.09% quantifies such anharmonicity by a value of $m \simeq 0.4$, with m being the parameter appearing in the elliptic Jacobi function [18]. Such parameter can range between zero (case of a circular cycloid, i.e, where anharmonicity is absent) and 1 (case of a square wave in which the spins bunch along the one of the coordinate axes). Our predicted value of about 0.4 is in-between the measured values of 0.25 and 0.53 found by neutron diffractions at low temperature in Refs. [18, 19]. Our simulations thus contrasts with the low-temperature NMR measurements providing a value of 0.95 for the Jacobi function parameter at 5K [15–17], and therefore tell

us that the magnetic cycloid of BFO possesses a rather low anharmonicity – in agreement with Refs. [18–21]. We also numerically found that the anharmonicity decreases as the C_{ij} coefficient of Eq. (1) increases at a fixed, low temperature.

We also investigated how the magnetic cycloid evolves when placed under a magnetic field, \mathbf{H} , aligned along $[\bar{2}11]$. Figure 3(a) displays the magnitude, M , of the resulting magnetization as a function of the strength, H , of the magnetic field, when choosing $C_{ij} = 4 \times 10^{-6}$ Hartree/(Bohr μ_B^2) and $T=5\text{K}$. Figure 3 (b) shows the corresponding evolution of the square of the Fourier transforms of the local magnetic dipoles configuration at $\mathbf{k}_{\text{cyclo}}$ and at the \mathbf{k} -vector associated with the R -point of the cubic first Brillouin zone (i.e., $\mathbf{k}_R = \frac{\pi}{2a_{\text{lat}}}(\mathbf{x} + \mathbf{y} + \mathbf{z})$). The magnetic cycloid transforms into a spin-canted structure (possessing a large G-type AFM vector and a weak perpendicular magnetization) for a magnetic field around 7 Tesla when $C_{ij} = 4 \times 10^{-6}$ Hartree/(Bohr μ_B^2) and $T=5\text{K}$ (we numerically found that the critical magnetic field is sensitive to C_{ij} . As a result, one needs to slightly increase it to obtain the experimental critical field of around 20 Tesla [26]). Interestingly, interpolating down to 0 Tesla the M -versus- H straight line existing above 7 Tesla provides a value of the magnetization of $0.027 \mu_B$ – which is the value of the magnetization of the spin-canted structure under no field when switching off C_{ij} in Eq. (1). Such features are consistent with experiments [26]. They also emphasize that the spin-canting, weak FM structure of BFO and the magnetic cycloid are related to two different and competing energies, namely, the sixth and last terms of Eq. (1), respectively. Figure 3 further reports the M -versus- H curve when *switching off* the “spin-canting” K_{ij} coefficient of Eq. (1). The magnetic cycloid is still found to possess both an in-plane and out-of-plane modulation at low magnetic field, and is still destroyed for magnetic fields of the order of 7 Tesla when $C_{ij} = 4 \times 10^{-6}$ Hartree/(Bohr μ_B^2) and $T=5\text{K}$. However, the resulting high-field structure can be thought as being purely G-type AFM rather than being canted (since the resulting magnetization at high field is nearly zero). As a result, and unlike thought in Ref. [22], the existence of the out-of-plane modulation inherent to the cycloidal structure can *not* be considered as the precursor of (or the same effect as) the weak FM occurring in the spin-canted structure.

It is also important to realize that we numerically found that is the *competition* between the last term of Eq. (1) and the other terms of this Equation – at the exception of the first term (magnetic dipolar) and the sixth term (related to the spin-canting) – that gives rise to the cycloid and its associated characteristics (such as SDW, small anharmonicity,

etc...). As a matter of fact, the last term of Eq. (1) by itself does not want to form a long-period cycloid, but rather favors magnetic moments successively aligned along the [111] (polarization) direction and then along the $[0\bar{1}1]$ (\mathbf{e}_{ij}) direction, when moving along the direction spanned by \mathbf{e}_{ij} . Moreover, the introduction of this last term does *not* automatically guarantee the existence of a SDW and low anharmonicity. Such features naturally result here from the minimization of the total energy of Eq. (1) (that includes several energies). Furthermore, this last term is not related to the suggested and commonly used complex relativistic Lifshitz-like invariant that is associated with the product between polarization, antiferromagnetic vector and the gradient of the antiferromagnetic vector [23]. It rather involves a much simpler analytical form where the essential interactions are between second-nearest neighbors. In fact, the analytical form of the last term of Eq. (1) can be thought of as the *converse* spin-current-induction effect [39], as consistent with what stated for the cycloid of BFO in Refs. [6, 40]. As a matter of fact, the spin-current-induction model was recently introduced to reveal how a peculiar magnetic cycloidal structure can lead to the formation of a polarization, while here we discuss the reciprocal effect that the existence of a polarization causes the occurrence of a magnetic cycloid (note that the idea that the polarization-induced cycloid of BFO is the converse effect of a cycloid-induced polarization was also indicated in Ref. [41]). Knowing the energetic origins of the magnetic cycloid in BFO and its characteristics (such as low anharmonicity and spin-density waves) is essential to understand many important features, such as spin dynamics, electromagnons [27–29], the control of the magnetic cycloid by electric field [5–7], the effect of temperature and surface on magnetic properties, etc...[42].

-
- [1] G.A. Smolenskii, I.E. Chupis, *Sov. Phys. Usp.* **25**, 475 (1982).
 - [2] W. Eerenstein, N. D. Mathur, J. F. Scott, *Nature* **442**, 759 (2006).
 - [3] N.A. Spaldin, and M. Fiebig, *Science* **309**, 391 (2005).
 - [4] J.B. Neaton *et al*, *Phys. Rev. B* **71**, 014113 (2005).
 - [5] T. Zhao *et al*, *Nature Materials* **5**, 823 (2006).
 - [6] D. Lebeugle *et al*, *Phys. Rev. Lett.* **100**, 227602 (2008).
 - [7] S. Lee *et al*, *Phys. Rev. B* **78**, 100101 (2008).

- [8] H. Bea *et al*, *Appl. Phys. Lett.* **87**, 072508 (2005); H. Bea *et al*, *Philos. Mag. Lett.* **87**, 165 (2007).
- [9] R. Haumont *et al*, *Phys. Rev. B* **73**, 132101 (2006).
- [10] C. Ederer and N.A. Spaldin, *Phys. Rev. B* **71**, 060401 (2005).
- [11] I. Kornev *et al*, *Phys. Rev. Lett.* **99**, 227602 (2007).
- [12] D. Albrecht, S. Lisenkov, Wei Ren, D. Rahmedov, Igor A. Kornev and L. Bellaiche, *Phys. Rev. B* **81**, 140401(R) (2010).
- [13] I. Sosnowska *et al*, *Physica B* **180**, 117 (1992).
- [14] I. Sosnowska, T. Peterlin-Neumaier and E. Steichele, *J. Phys. C: Solid State Phys.* **15**, 4835 (1982).
- [15] A.V. Zalesskii *et al*, *JETP* **95**, 101 (2002).
- [16] A.V. Zalesskii *et al*, *JETP Lett.* **71**, 465 (2000).
- [17] A.A. Bush *et al*, *JETP Lett.* **78**, 389 (2003).
- [18] M. Ramazanoglu *et al*, *Phys. Rev. B* **83**, 174434 (2011).
- [19] I. Sosnowska and R. Przenioslo, *Phys. Rev. B* **84**, 144404 (2011).
- [20] R. Przenioslo *et al*, *J. Phys. Cond. Mat* **18**, 2069 (2006).
- [21] V. S. Pokatilov and A. S. Sigov, *Journal of Experimental and Theoretical Physics* **110**, 440 (2010).
- [22] M. Ramazanoglu *et al*, *Phys. Rev. Lett.* **107**, 207206 (2011).
- [23] I. Sosnowska and A.L. Zvezdin, *Journal of Magnetism and Magnetic Materials* **140-144** 167 (1995).
- [24] R. de Sousa and J. E. Moore, *Appl. Phys. Lett.* **92**, 022514 (2008).
- [25] J. Jeong *et al*, *Phys. Rev. Lett.* **108**, 077202 (2012).
- [26] D. Wardecki *et al*, *J. Phys. Soc. Jpn.* **77**, 103709 (2008).
- [27] D. Talbayev *et al*, *Phys. Rev. B* **83**, 094403 (2011).
- [28] M. Cazayous *et al*, *Phys. Rev. Lett.* **101**, 037601 (2008).
- [29] P. Rovillain *et al*, *Nature Materials* **9**, 975 (2010).
- [30] W. Zhong, D. Vanderbilt and K.M. Rabe, *Phys. Rev. Lett.* **73**, 1861 (1994); *Phys. Rev. B* **52**, 6301 (1995).
- [31] I. Kornev *et al*, *Phys. Rev. Lett.* **97**, 157601 (2006).
- [32] P. Fischer *et al*, *J. Phys. C* **13**, 1931 (1980).

- [33] S. Lisenkov, Igor A. Kornev and L. Bellaiche, *Phys. Rev. B* **79**, 012101 (2009); *Phys. Rev. B* **79**, 219902(E) (2009).
- [34] One difficulty for atomistic simulations to capture the precise characteristics of the observed magnetic cycloid in BFO is related to its large period of the order of 63 nm [6, 13, 14, 18, 22]. Such length is too large to be handled with atomistic methods. However, our main objective is to reproduce and understand important *qualitative* rather than purely quantitative features of this cycloid. Examples of such qualitative features are its anharmonicity [15–18], the existence of out-of-plane spin-density waves superimposed to an in-plane cycloid propagating along a specific direction in a plane containing the polarization [22], and its annihilation by a magnetic field [26]. We thus decided to focus on a $18 \times 18 \times 18$ supercell (which possesses lateral sizes of the order of 7 nm and contains 29,160 atoms) to model bulk BFO.
- [35] S.V. Kiselev *et al*, *Sov. Phys. Dokl.* **7**, 742 (1963); G.A. Smolenskii *et al*, *Sov. Phys. Solid State* **2**, 2651 (1961).
- [36] J.R. Teague, R. Gerson and W.J. James, *Solid State Comm.* **8**, 1073 (1970).
- [37] We analytically found that the C_{ij} coefficient leading to the measured period of the cycloid [6, 13, 14, 18, 22] is around 4.3×10^{-6} Hartree/(Bohr μ_B^2), if one uses the *ab-initio-derived* parameters entering Eq. (1). Note that such value is above the critical value of $\simeq 3 \times 10^{-6}$ Hartree/(Bohr μ_B^2), that allows the cycloid to be more energetically favorable than the spin-canted solution.
- [38] A.M. George, J. Iñiguez and L. Bellaiche, *Phys. Rev. B* **65**, 180301 (R) (2002).
- [39] H. Katsura, N. Nagaosa and A.V. Balatsky, *Phys. Rev. Lett.* **95**, 057205 (2005).
- [40] A. M. Kadomtseva, A. K. Zvezdin, Y. F. Popov, A. P. Pyatakov, G. P. Vorobev, *JETP Lett.* **79**, 571 (2004).
- [41] G. Catalan and J.F. Scott, *Adv. Mater.* **21**, 2463 (2009).
- [42] This work is mostly financially supported by the NSF grants DMR-1066158 and DMR-0701558. We also acknowledge Department of Energy, Office of Basic Energy Sciences, under contract ER-46612, ARO Grant W911NF-12-1-0085 and ONR Grants N00014-11-1-0384 and N00014-08-1-0915 for discussions with scientists sponsored by these grants. D.W. acknowledges support from the National Natural Science Foundation of China under Grant No. 10904122. J.I. acknowledges funding from MICINN-Spain (Grants No. MAT2010-18113 and No. CSD2007-00041). Some computations were also made possible thanks to the MRI grant

0722625 from NSF, the ONR grant N00014-07-1-0825 (DURIP) and a Challenge grant from the Department of Defense. We are also grateful to D. Lebeugle, D. Albrecht, A. Barthélemy, M. Bibes, B. Dkhil and I. Kornev for many discussions.

FIGURE CAPTIONS

Figure 1: Snapshot of the magnetic dipoles configurations at 0.2K when the C_{ij} parameter of Eq. (1) is chosen to be 5×10^{-6} Hartree/(Bohr μ_B^2). Panel (a) shows the projections of the magnetic dipoles into the $(\bar{2}11)$ cycloidal plane for a line of dipoles centered along the same $[0\bar{1}1]$ direction. Panel (b) displays the out-of-plane components of these dipoles.

Figure 2: Angle made by the magnetic dipoles with the polarization (open squares) and angle made by these dipoles out of the cycloidal plane (open circles), for a line of dipoles centered along the same $[0\bar{1}1]$ direction. C_{ij} is chosen to be 5×10^{-6} Hartree/(Bohr μ_B^2) and the temperature is 0.2K. The horizontal dashed line corresponds to zero angles.

Figure 3: Magnitude of the magnetization (Panel a) and of the square of the Fourier transforms of the local magnetic dipoles's configuration (Panel b) at $\mathbf{k}_{\text{cyclo}}$ (circles) and $\mathbf{k}_{\mathbf{R}}$ (squares), as a function of the magnitude of the magnetic field applied along the $[\bar{2}11]$ direction when the K_{ij} parameter of Eq. (1) is switched on (open symbols) or off (filled symbols). The C_{ij} parameter of Eq. (1) is chosen to be 4×10^{-6} Hartree/(Bohr μ_B^2) and the temperature is 5K. The dashed line in Panel (a) shows the interpolation down to 0 Tesla of the M-versus-H straight line existing above 7 Tesla when K_{ij} is switched on.

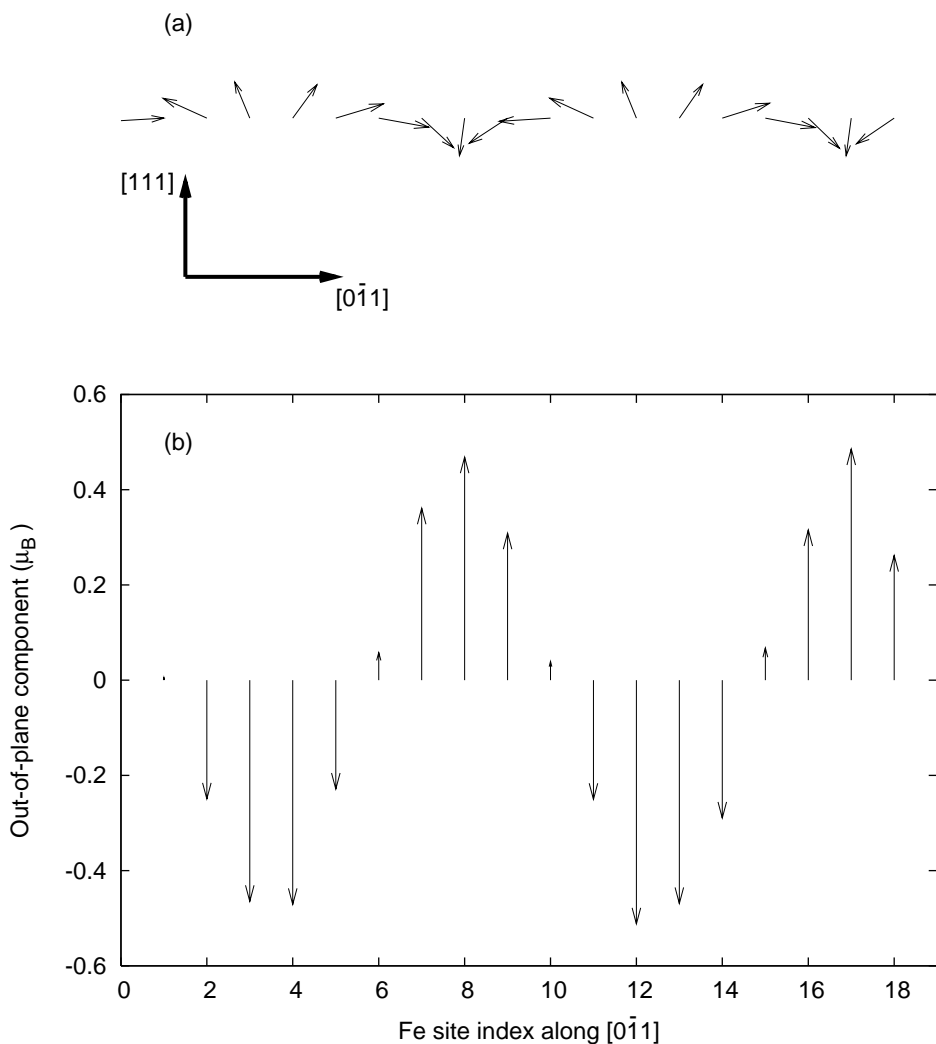


Figure 1 LP13250 18Jun2012

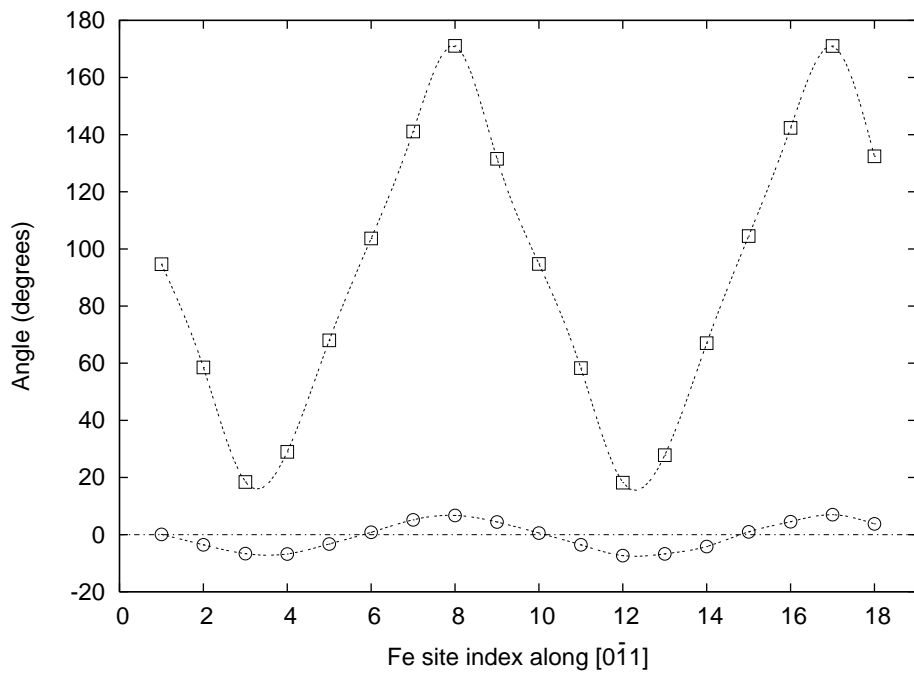


Figure 2 LP13250 18Jun2012

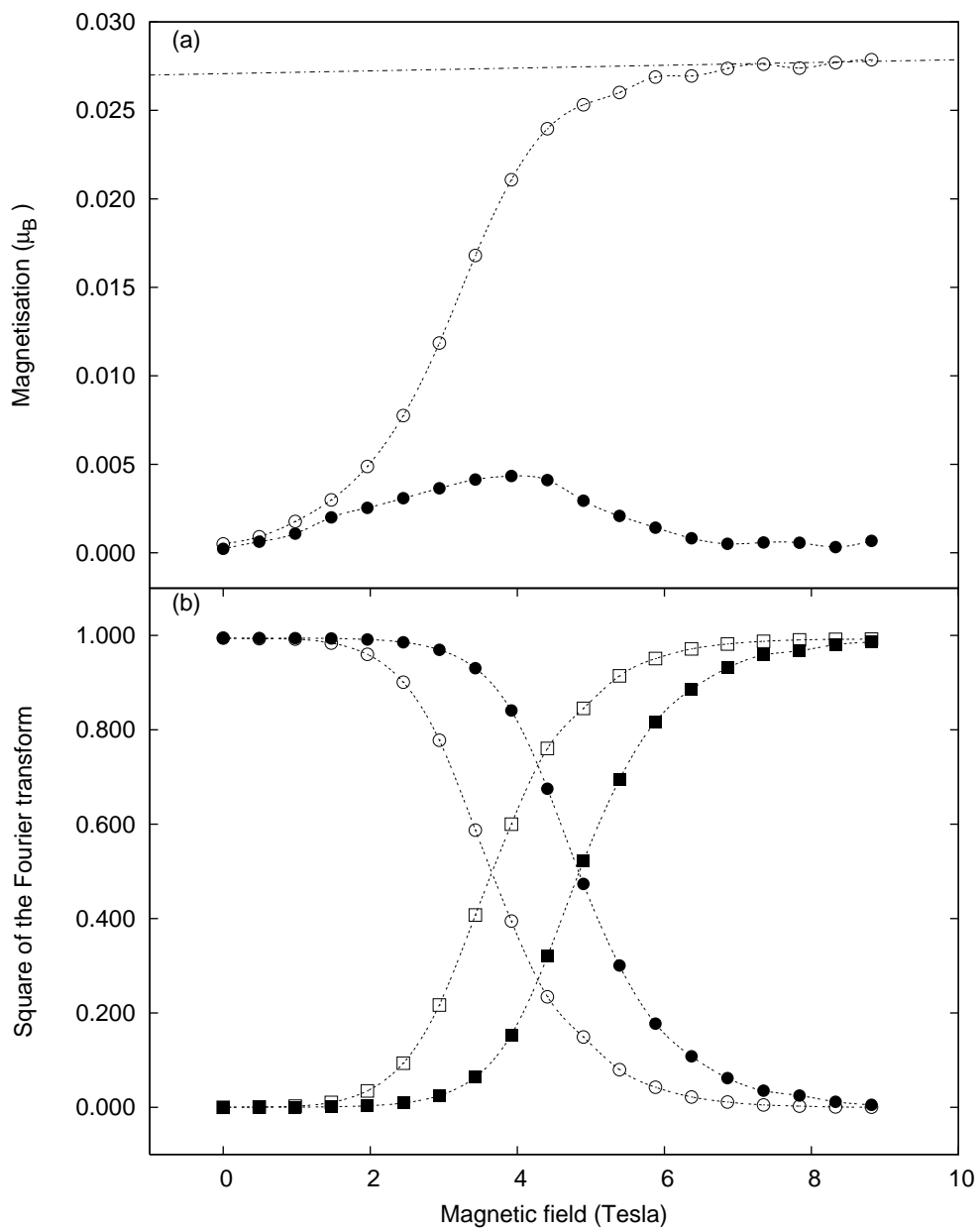


Figure 3 LP13250 18Jun2012